UNIVERSITY OF BIRMINGHAM
University of Birmingham Research at Birmingham

Comparison of Chromia Growth Kinetics in a Ni-based Superalloy, with and without Shot-peening

Cruchley, S.; Taylor, Mary; Ding, Rengen; Evans, Hugh; Child, D.J.; Hardy, M.C.

DOI:
10.1016/j.corsci.2015.07.033

License:
Creative Commons: Attribution-NonCommercial-NoDerivs (CC BY-NC-ND)

Document Version
Peer reviewed version

Citation for published version (Harvard):
Cruchley, S, Taylor, M, Ding, R, Evans, H, Child, DJ & Hardy, MC 2015, 'Comparison of Chromia Growth Kinetics in a Ni-based Superalloy, with and without Shot-peening', *Corrosion Science*, vol. 100, pp. 242-252. https://doi.org/10.1016/j.corsci.2015.07.033

Link to publication on Research at Birmingham portal

Publisher Rights Statement:
Eligibility for repository: Checked on 11/09/2015

General rights
Unless a licence is specified above, all rights (including copyright and moral rights) in this document are retained by the authors and/or the copyright holders. The express permission of the copyright holder must be obtained for any use of this material other than for purposes permitted by law.

•Users may freely distribute the URL that is used to identify this publication.
•Users may download and/or print one copy of the publication from the University of Birmingham research portal for the purpose of private study or non-commercial research.
•User may use extracts from the document in line with the concept of 'fair dealing' under the Copyright, Designs and Patents Act 1988 (?)
•Users may not further distribute the material nor use it for the purposes of commercial gain.

Where a licence is displayed above, please note the terms and conditions of the licence govern your use of this document.

When citing, please reference the published version.

Take down policy
While the University of Birmingham exercises care and attention in making items available there are rare occasions when an item has been uploaded in error or has been deemed to be commercially or otherwise sensitive.

If you believe that this is the case for this document, please contact UBIRA@lists.bham.ac.uk providing details and we will remove access to the work immediately and investigate.

Download date: 19. Apr. 2024

Accepted Manuscript

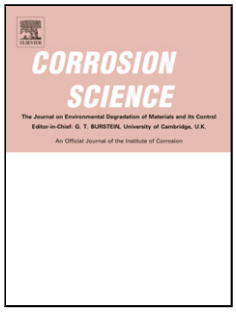

Title: Comparison of Chromia Growth Kinetics in a Ni-based Superalloy, with and without Shot-peening

Author: S. Cruchley M.P. Taylor R. Ding H.E. Evans D.J. Child M.C. Hardy

PII: S0010-938X(15)30030-5
DOI: http://dx.doi.org/doi:10.1016/j.corsci.2015.07.033
Reference: CS 6426

To appear in:

Received date: 4-3-2015
Revised date: 16-7-2015
Accepted date: 31-7-2015

Please cite this article as: S.Cruchley, M.P.Taylor, R.Ding, H.E.Evans, D.J.Child, M.C.Hardy, Comparison of Chromia Growth Kinetics in a Ni-based Superalloy, with and without Shot-peening, Corrosion Science http://dx.doi.org/10.1016/j.corsci.2015.07.033

This is a PDF file of an unedited manuscript that has been accepted for publication. As a service to our customers we are providing this early version of the manuscript. The manuscript will undergo copyediting, typesetting, and review of the resulting proof before it is published in its final form. Please note that during the production process errors may be discovered which could affect the content, and all legal disclaimers that apply to the journal pertain.

ACCEPTED MANUSCRIPT

Comparison of Chromia Growth Kinetics in a Ni-based Superalloy, with and without Shot-peening

S. Cruchley[a] (S.Cruchley@pgr.bham.ac.uk), M.P. Taylor[a*] (M.P.Taylor@bham.ac.uk), R. Ding[a] (R.Ding@bham.ac.uk), H.E. Evans[a] (H.E.Evans@bham.ac.uk), D.J. Child[b] (Daniel.Child@Rolls-Royce.com) and M.C. Hardy[b] (Mark.Hardy@Rolls-Royce.com)

[a]School of Metallurgy and Materials, University of Birmingham, Birmingham, B15 2TT, UK

[b]Rolls-Royce plc, Derby, DE24 8BJ, UK

*corresponding author

Keywords: Superalloys, Oxidation, Selective oxidation.

Highlights

- Two alloy surface treatments are compared.
- The kinetics of a Ni-based superalloy are compared to pure chromia formation.
- The enhancement is described in terms of Ti-doping of the surface chromia scale.
- For the first time, a $(Ta,Ti)O_2$ phase, formed at the oxide metal interface, is identified.

Abstract

The effect of shot-peening on the oxidation in air of the Ni-based superalloy RR1000 has been investigated over the temperature range 700-800^{o}C. The surface oxide in both peened and un-peened conditions consisted of isolated grains of rutile on the outermost surface beneath which was a protective Ti-doped chromia scale. Internal oxidation of aluminium occurred within the alloy with the formation of alumina particles within a γ (nominally $Ni_3(Al,Ti)$) denuded zone but the morphology of the sub-surface oxides differed between the two surface conditions examined. The kinetics of thickening of the chromia layer were sub-parabolic in most cases but closely approached parabolic behaviour for the un-peened surface condition at 800^{o}C. An enhancement in the rate of chromia growth was found for both surface conditions compared with a Ti-free chromia layer. This enhancement has been attributed to increased Cr ion diffusion as a result of Ti-doping of the chromia layer but the effect is reduced over time because of Ti-depletion in the alloy. At 800^{o}C, in the un-peened condition, the reduction in growth rate with exposure time is much less marked and this effect seems to be associated with the formation of a $(Ti,Ta)O_2$ phase beneath the chromia layer.

Introduction

ACCEPTED MANUSCRIPT

High temperature oxidation resistance is becoming increasingly important as operating temperatures increase, particularly in aero-engines. This is in response to the need to improve fuel efficiency and reduce harmful emissions. It has been established that shot-peening can extend the service life of critical components through inducing compressive stresses in the surface and thereby improving fatigue crack resistance [1, 2]. This process is commonly used on rotor discs in service. Little work has previously been performed to investigate the oxidation characteristics of Ni-based superalloys having undergone shot-peening or similar surface modifications. Most studies have been performed on material with either as-machined or polished surfaces but it is important that the oxidation damage is evaluated on the actual surface condition that is used on the component in service. By contrast, the oxidation behaviour of Ni-based superalloys [3-8], and specifically RR1000 [9-13] in the polished/machined condition, has been studied extensively and has been the subject of a number of recent publications. Typically during high temperature exposure of specimens in laboratory tests, a continuous surface layer of chromia is formed but with isolated particles of TiO_2 on the outer surface. Internal oxidation of aluminium also occurs and results in the formation of sub-surface precipitates of alumina [3, 4, 9, 12]. Ahead of this zone of internal oxidation lies a region depleted in γ' (nominally $Ni_3(Al,Ti)$) precipitates and, after oxidation in air at temperatures >800^{o}C, precipitates of TiN [9, 10]. A grain boundary carbide ($M_{23}C_6$) depleted region underneath the surface oxide has also been reported in a similar Ni-based superalloy, ME3, [4] and similar observations have been made in RR1000 [10]. Sigma phase formation in such alloys is also possible [14].

Shot-peening is expected to enhance chromium diffusion in the near surface region of the alloy, through an increase in dislocation density, and result in the quicker formation of a protective Cr-rich surface oxide layer. This has been demonstrated for boiler steels and for the Fe-Ni based alloy 800H [15, 16]. However, shot peening has also been shown to increase oxidation rates in alloys where protective oxide scales are normally found. This is the case in previous work investigating the weight gain kinetics of RR1000 where it was shown that shot-peening had an adverse effect on oxidation at 700 and 750^{o}C [17].

The present work provides a more detailed comparison of the oxidation response of the two surface conditions through extensive measurements of oxide layer thickness. The work complements an earlier study [11] on the un-peened RR1000 alloy and detailed comparison

ACCEPTED MANUSCRIPT

with these earlier data will be made in the present work. The earlier work conducted on this alloy by the same authors recorded the mass-gain oxidation kinetics [9, 11, 17], sub-surface oxidation kinetics [10]. As part of the detailed investigation performed the presence of Ti within the chromia was noted [11]. The analysis of the kinetics of the external chromia growth was performed using extensive metallographic measurements. The chromia growth on this alloy was found to be significantly greater than that observed previously on Ti-free chromia. From this observation a mechanism for sub-parabolic growth of this chromia scale was produced and attributed to increased ionic transport caused by the doping of the chromia scale by Ti [18].

In this paper, particular attention will be paid to the influence of shot peening on the kinetics of thickening of the chromia layer. The role of Ti on this process will also be considered.

Experimental Procedure

An advanced powder metallurgy Ni-based superalloy, RR1000, was used in this study and was provided by Rolls-Royce plc. The nominal composition is given in Table I. The alloy consists principally of a two-phase microstructure of a γ (nominally Ni, Co) matrix and approximately a 45% volume fraction of γ' precipitates.

The material was prepared with either a polished or shot-peened surface condition. For the former, samples were cut (10 mm x 5 mm x 2 mm), ground and the edges chamfered before being polished to a 6 μm finish (Ra= 0.3 μm) using conventional preparation methods. For the shot-peened condition, the same batch of alloy was again cut to provide samples (20 mm x 10 mm x 2 mm), whose edges were chamfered and the large surfaces ground to a 1200 grit finish. These specimens were then shot-peened using the following conditions: 110H steel shot, 6-8 Almen and 200% coverage.

Oxidation testing was conducted over the temperature range of 700 to 800°C in laboratory air for times up to 8000h in the polished condition and 2000h in the shot-peened condition. Prior to testing, the specimens were cleaned in ethanol and dried, before being placed in batches into alumina boats and inserted into horizontal tube furnaces at temperature. The furnace was previous calibrated using an N-type thermocouple to $\pm 1^{o}$C. At selected time intervals, a specimen was removed from the batch for examination before the high temperature exposure

ACCEPTED MANUSCRIPT

continued for the remainder of the batch. Table II shows the time intervals chosen for examination.

After oxidation testing, both surface and cross-sectional examination was performed. The surfaces of the specimens were sputter coated with gold and examined by scanning electron microscopy (SEM) using both secondary (SE) and backscattered electrons (BSE). Cross-sectional analysis was performed by nickel-plating the specimens before they were mounted using vacuum impregnation in a low viscosity resin. The specimens were prepared for cross-sectional analysis by grinding on SiC papers down to 1200 grit using water as a lubricant followed by polishing using progressively finer diamond paste from 6 μm down to 0.25 μm. The cross-sections were examined using a high resolution JEOL 7000F FEGSEM. This equipment is capable of wavelength dispersion spectroscopy (WDS), used here for the identification of oxygen, nitrogen and carbon, and energy dispersion spectroscopy (EDS) used for heavier element compositional identification, mapping and line scans. X-ray diffraction (XRD) analysis of the surface oxides was performed on a Philips XPert system using Cu Kα radiation, indexed between a 2θ of 10-100º. Metallographic measurements of chromia thicknesses were performed, as described elsewhere [11], using a total of 50 measurements taken from 10 micrographs of representative images of each specimen as shown in Figure 1. EDS analysis was used to confirm that the measurement conformed to just the chromia part of the external scale.

Thin sections for transmission electron microscopy were produced using focussed ion beam sectioning on a Quanta 3D FEG FIB/SEM dual beam system. EDS compositional analysis and selected area diffraction were then undertaken using a field emission gun Tecnai F20 (S)TEM.

Results and Discussion

Oxide characterisation

The typical oxide morphology (both surface and internal) of both polished and shot-peened RR1000 is shown in the cross-sections of Figure 1. EDS analysis confirmed that the external oxides were chromium and titanium rich and that sub-surface alumina was formed (Figure 2a). XRD analysis confirmed that the composition of the surface oxide was the same in both shot-peened and polished RR1000, being comprised of chromia and rutile (Table III). XRD

ACCEPTED MANUSCRIPT

analysis could not detect sub-surface oxides with confidence because of their depth within the alloy and their relatively small volume fraction.

The EDS map of oxidised shot-peened RR1000 indicates that rutile exists as isolated particles located on the outer surface of the chromia scale but it also shows that detectable quantities of Ti are present throughout the chromia layer (Figure 2a). In the previous paper [11] on un-peened material, Ti was also found within the chromia layer but it is known [18] that appreciable solubility of Ti is possible without significant changes to the chromia lattice spacing, as measured by XRD. Within this external oxide scale, for both initial surface conditions, are entrapped particles rich in Ni and Co. This protrusion formation has been described previously [10, 11] and is either developed via undercutting by oxide formation [19] or by outward alloy creep to accommodate the stress caused by the increase in volume resulting from internal oxide formation [20-24]. In addition, a few isolated voids were present in the external oxide for both initial surface conditions.

Underneath the external oxide scale, at the alloy/external oxide interface, a (Ti,Ta)-rich phase was identified (Figure 2b) but this was only observed in specimens oxidised at 800^{o}C. In the long-term test (2000 hours), this phase was nearly continuous in the polished (un-peened) specimen but only fragmentary in the shot-peened specimen. EDS spot analyses (Figure 2b) could not produce unambiguous identification because of the small particle size and the likelihood that signals were also being obtained from the adjacent chromia layer. Accordingly, further analyses were undertaken on TEM samples produced by FIB sectioning of this surface region. A FIB section through the unidentified phase is shown in Figure 3a together with the external chromia layer (right-hand side), internal alumina precipitates and the alloy. The area EDS spectrum results obtained from the rectangular region shown in Figure 3 provide a more accurate composition for the phase of 20.6 Ti, 12.0 Ta, 4.2 Cr, 63.2 O at.%, which corresponds approximately to the MO_2 rutile stoichiometry. The higher resolution capability of TEM gives a more precise composition for the phase due to the small interaction area than that provided using SEM. Studies on the Ni-based superalloy ME3 [4] have also reported the presence of a rutile-type phase underlying the outer chromia layer but, in that case, the major metallic constituents were reported to be Ti and Cr. To provide further insight, Selective Area Diffraction (SAD) patterns were obtained from the unidentified phase marked in Figure 3 and these are shown in Figure 4. These confirm that the phase has a tetragonal rutile-type structure with ‘a’=0.47 nm and ‘c’=0.30 nm. For comparison, rutile

ACCEPTED MANUSCRIPT

(TiO_2) has 'a'=0.46 nm and 'c'=0.295 nm [24]. TaO_2 has a similar crystallographic structure with 'a'=0.47 nm and 'c'=0.31 nm [24]. These values agree closely with those measured here and so it seems likely that the phase is $(Ti,Ta)O_2$. Whether or not Cr is actually present is unclear because of the possibility of signal contamination from the adjacent chromia layer during the EDS scan.

Sub-surface internal oxides precipitate in different morphologies depending on the initial surface condition and grain structure (Figure 1). In the polished (un-peened) condition, the alumina intrusions form both intergranularly and intragranularly, with the former being deeper and more acicular in nature. In the shot-peened condition a more uniform depth of internal oxidation exists as a result of alumina formation predominantly at the grain boundaries of small recrystallized grains that form in the near-surface region. An example is shown in Figure 5 from which it can be seen that the size of these grains is approximately 1-3 µm. This compares with the 30-50 µm grain size of the bulk alloy. The maximum depth of internal oxidation is similar for both initial surface conditions, however, indicating that shot peening and subsequent recrystallization has not affected the rate of supply of the reacting species (Al and O). The γ′ denuded zone lies ahead of the internal oxidation front but tends to follow the contours of the latter, Figure 1. The depth of the γ′-denuded zone is more uniform in the shot-peened specimens than in the polished (Figure1) but the maximum depth of depletion is similar in both.

Chromia growth kinetics

As previously described the mass gain kinetics of RR1000 with and without shot-peening have shown that, at 700°C and 750°C, a significant detrimental effect of shot-peening exists [17]. Since more than one element is oxidising in the case of RR1000, it is unclear whether this increased mass gain came from the enhanced formation of the external chromia scale or whether it is related to the depth and volume of the internal oxides or to the formation of rutile. It is for this reason that extensive measurements of chromia thickness were undertaken in the present work.

Figure 6 shows the chromia thickness against exposure time at the three principal test temperatures for both shot-peened and polished RR1000. The scatter shown represents a ±1 standard deviation of the 50 measurements taken from each specimen. The shot-peened data

ACCEPTED MANUSCRIPT

at 750°C have been published in an earlier paper [11] but inadvertently described there as being for the polished specimens. This regrettable error has been corrected in the present paper. The lines drawn through the RR1000 data in Figure 6 represent best fits to Equation (1):

$$\xi = (k_m t)^{1/m} \quad (1)$$

where k_m is an effective rate constant, ξ is oxide thickness, m is a numerical constant and t is exposure time. The values for k_m and m are given in Table IV from which it can be appreciated that, in all cases, sub-parabolic kinetics are obtained ($m > 2$) although for the polished material tested at 800°C parabolic behaviour is closely approached. Sub-parabolic kinetics have also recently been reported for the similar Ni-based superalloy, ME3 [14]. From Figure 6, it can be appreciated that there does not seem to be a consistent trend in the comparison between the initial surface conditions. Thus, the trend of the means, and hence the best-fit lines, at both 700 and 750°C is that the rate of chromia growth on the shot-peened specimens is higher than on the polished equivalent but only marginally so at 700°C. At 800°C a converse trend exists in that shot-peening appears to provide benefit. A comparison between the means at 2000-hours exposure at each temperature was made using the t-test (with different variances between the data sets) to check for significance. It was found that the difference between the means at all three temperatures was significant ($p<0.05$): the probability that the difference in means occurred by chance was (to 3 decimal places) 0.041 at 700°C and 0.000 at both 750 and 800°C.

For both initial surface conditions, the rate of thickening of the chromia layer is enhanced over that expected for growth of an adherent chromia layer on pure chromium or on a simple austenitic steel. The lower solid line in each of the plots in Figure 6 applies to parabolic chromia growth on these materials and is given by Equations (2) and (3) [26]:

$$k_p = 2.07 \times 10^{-6} \exp\left[-\frac{31020}{T}\right], \ \mathrm{m^2 s^{-1}} \quad (2)$$

$$\xi = (k_p t)^{1/2} \quad (3)$$

ACCEPTED MANUSCRIPT

where T is absolute temperature, k_p is the parabolic rate constant, ξ is chromia layer thickness and t is exposure time. The enhancement in chromia growth rate in the RR1000 superalloy over that predicted by Equations (2) and (3) can be quantified, as previously [11], from the ratio, r, of the slopes, $d\xi/dt$, of the respective chromia-thickness/time curves (Equation (4)). Note that the best-fit curves using the parameter given in Table IV were used in this comparison.

$$r = \left(\frac{(d\xi / dt)_s}{(d\xi / dt)_{cr}} \right)_{\xi} \tag{4}$$

Here, the subscript 's' refers to the superalloy and 'cr' to pure chromium or the simple austenitic alloy. The comparison needs to be made at a given chromia thickness so that the diffusion distance for the chromium defects transporting across the oxide layer is the same in each case. The dependence of the ratio 'r' on oxide thickness and test temperature is shown in Figure 7a for the polished and Figure 7b for the shot-peened alloy.

Clearly it can be recognised that, at 700°C and 750°C, the enhancement ratio shows a similar trend for both initial surface conditions in that for thin oxide scales (~0.1-0.2 µm), a 2 orders of magnitude increase in growth rate was found. As the scale thickens, this reduces in both cases to an enhancement ratio of ~10. At 800°C, similar enhancement factors (~10) for thicker scales (>1 µm) exist for both polished and shot-peened conditions but the large values found for thin oxides at 700 and 750°C were present only for the shot-peened condition at 800°C. Close examination of the early stage kinetics, Figure 6, at 800°C shows little difference with the two data sets following a similar trend up to 200 hours and thus one would expect this to be reflected in the enhancement ratios. However, the oxidation kinetics has been determined from the whole data set and this includes data extending well beyond 200 hours, Figure 6. The constant enhancement ratio at 800°C for the polished condition is a reflection that parabolic kinetics are maintained over the test period and an explanation, involving the influence of the $(Ti,Ta)O_2$ phase, is incorporated into the doping mechanism, and is given below.

The enhancement of the growth rate of the chromia scale has previously been explained by an increase in chromium vacancies as a result of the incorporation of the higher-valent Ti^{4+} ion leading to an increase in the oxidation rate through increased diffusion rates of chromium

ACCEPTED MANUSCRIPT

ions across the oxide [11, 27-31]. This mechanism is also expected to apply to the shot-peened condition tested here. As the oxide thickens and depletion of Ti underneath the external oxide scale ensues, the flux of Ti into the oxide scale is reduced and the average Ti concentration in the chromia layer is also reduced. This causes a corresponding reduction in the rate-enhancement ratio as the oxide thickness increases (Figure 7a and 7b).

This alloy depletion of Ti at 750^{o}C is illustrated by the SEM and EDS line scans shown in Figures 8 (reproduced from [11] for completeness) and 9 for the polished and shot-peened alloy, respectively. The locations of the external oxides, γ' denuded zones and the alloy are labelled in each EDS linescan. For the polished specimen after 100 hours exposure (Figure 8a), it can be seen that within the γ' denuded zone there is some depletion of both Ti and Al although, adjacent to the external oxide scale, there is also an enhancement of Al, probably associated with alumina. The presence of Ti within the chromia scale is also evident but not rutile on the outer surface of the chromia layer for the section examined. After 2000 hours oxidation at 750^{o}C (Figure 8b), rutile is present as the outermost oxide. Ti depletion of the γ' denuded zone is more advanced than after 100 hours and the rate of supply of Ti into the chromia layer is also expected to be less since its concentration gradient into the oxide layer is also reduced. These observations are consistent with the qualitative model described above for the development of sub-parabolic chromia growth kinetics in this alloy, at least at 700 and 750^{o}C. Somewhat tentatively, an estimate of the Ti/Cr ratio within the chromia layer can be made by comparing the Ti and Cr counts at the peak of the Cr counts. It is found for the polished alloy (Figure 8) that after 100 hours at 750^{o}C, Ti/Cr ~ 0.22 but this is reduced to ~0.14 after 2000 hours. The same trend is found for the shot-peened alloy (Figure 9) where Ti/Cr ~ 0.22 after 100 hours and 0.14 after 2000 hours. Note that the peaks in Ti and Al within the depletion zone at these long exposure times appear to be associated with nitride and oxide particles.

Similar trends to those described above appear also to exist for the specimens oxidised at 800^{o}C although the formation of nitride and oxide phases within the depletion zone and the early formation of rutile on the outer surface of the chromia layer makes numerical comparisons unreliable. A significant feature appears to be the presence of the (Ti, Ta)O_2 phase discussed earlier (e.g. Figures 3 and 4). This is present at this temperature for both surface conditions but only in significant quantities in the polished specimens. Its formation

ACCEPTED MANUSCRIPT

may limit Ti ingress into the chromia layer and, thus, reduce the doping effect at short times, i.e. up to 200 hours, (Figure 7) but sustaining that effect over longer time period leading to near-parabolic kinetics in the polished specimens at 800^{o}C to in excess of 2000 hours. It is postulated that the (Ta,Ti)O_2 phase forms at the oxide alloy interface but in the polished condition the phase forms a near continuous layer whereas the effect of the shot peening results in a discontinuous distribution of that phase. The phase, located as it is immediately beneath the external scale, will affect the diffusion of chromium to the surface and possibly result in a slower release of Ti ions into the chromia scale. In this way, the chromia scale growing on the polished samples at 800^{o}C are doped at a slower but continuous rate over the test periods used here and hence maintains parabolic growth kinetics.

An apparently consistent difference between the polished and shot-peened specimens is in the Cr depletion profiles. Those for the polished specimen at 750^{o}C (Figure 8) show a monotonic decrease in Cr concentration from the bulk alloy through the depletion zone towards the oxide/metal interface. By contrast, the shot-peened alloy shows an enhanced Cr concentration within the γ' denuded zone at both short (100 hours) and long (2000 hours) exposure times (Figure 9). This trend is also clear for oxidation at 800^{o}C as shown in Figures 10 and 11 for the polished and shot-peened alloys, respectively. This difference between shot-peened and peened regions has not previously been reported in this or similar chromia-forming Ni-based superalloys and merits further study.

Conclusions

The oxidation damage of RR1000 with and without shot-peening has been investigated over the temperature range of 700-800^{o}C for exposure times up to 2000 hours. A detailed comparison has been drawn between the two conditions as well as with oxidation of pure chromium. The main findings of the work are summarised below.

1. The oxide formed in air at all test temperatures (700, 750 and 800^{o}C) and in both surface conditions consists of a surface scale of chromia with isolated particles of rutile on the outer surface. Sub-surface alumina precipitates in a different morphology depending on the surface condition. For the polished specimens, intergranular oxidation penetrates to greater depths than the oxides formed within the alloy grains. For the shot-peened condition, the sub-surface oxide penetration occurs to a more

ACCEPTED MANUSCRIPT

uniform depth and tends to be associated with the grain boundaries of small recrystallised grains. Recrystallisation is found only in the shot-peened condition. A γ' denuded zone is present ahead of the zone of internal oxidation for both alloy conditions.

2. The growth rate of the chromia scale on shot-peened RR1000 was sub-parabolic in all cases as well as on the polished alloy at 700^{o}C and 750^{o}C. For these cases, there is a large (two orders of magnitude) enhancement in chromia growth rate for thin layers (~0.1 µm) over that expected for pure chromia. This enhancement factor declines as the oxide thickens. The increased oxidation rate is attributed to increased ionic transport caused by doping of the chromia layer by titanium and the consequent creation of vacancies on the chromium sub-lattice. The reduction in enhancement with increasing thickness occurs due to Ti depletion of the underlying alloy.

3. At 800^{o}C in the polished condition, the early-stage enhancement is much less (~ a factor of 10) but does not reduce substantially with increasing oxide thickness. As a consequence, the oxide growth kinetics are nearly parabolic for this one test condition. At this test temperature of 800^{o}C a (Ti, Ta)O_2 forms at the oxide/metal interface and may reduce the transport of Ti into the chromia layer extending the time period over which doping occurs.

4. For the polished specimens oxidised at 750 and 800^{o}C (the two temperatures at which detailed EDS analysis was undertaken), a Cr-depletion profile extends monotonically beyond the γ' denuded zone into the alloy. This is not the case for the shot-peened specimens where an enhancement of Cr concentration exists within this depleted zone.

Acknowledgements

The authors are grateful for the financial support of the Engineering and Physical Sciences Research Council and of Rolls-Royce plc through the Strategic Partnership Programme Work Package 3.2.

References

ACCEPTED MANUSCRIPT

[1] B.J. Foss, S. Gray, M.C. Hardy, S. Stekovic, D.S. McPhail, B.A. Shollock, Analysis of shot-peening and residual stress relaxation in the nickel-based superalloy RR1000, Acta Materialia, 61 (2013) 2548-2559.

[2] D.J. Child, G.D. West, R.C. Thomson, Assessment of surface hardening effects from shot peening on a Ni-based alloy using electron backscatter diffraction techniques, Acta Materialia, 59 (2011) 4825-4834.

[3] J. Chen, P. Rogers, J.A. Little, Oxidation behavior of several chromia-forming commercial nickel-base superalloys, Oxidation of Metals, 47 (1997) 381-410.

[4] C.K. Sudbrack, S.L. Draper, T.T. Gorman, J. Telesman, T.P. Gabb, D.R. Hull, Oxidation and the effects of high temperature exposures on notched fatigue life of an advanced powder metallurgy disk superalloy, in: E.S. Huron, R.C. Reed, M.C. Hardy, M.J. Mills, R.E. Montero, P.D. Portella, J. Telesman (Eds.) Superalloys 2012: 12th International Symposium on Superalloys, TMS, Seven Springs, PA, 2012, pp. 863-872.

[5] G.A. Greene, C.C. Finfrock, Oxidation of Inconel 718 in Air at High Temperatures, Oxidation of Metals, 55 (2001) 505-521.

[6] D. Kim, C. Jang, W. Ryu, Oxidation characteristics and oxide layer evolution of Alloy 617 and Haynes 230 at 900 °C and 1100 °C, Oxidation of Metals, 71 (2009) 271-293.

[7] B.R. Barnard, P.K. Liaw, R.A. Buchanan, D.L. Klarstrom, Affects of applied stresses on the isothermal and cyclic high-temperature oxidation behavior of superalloys, Materials Science and Engineering: A, 527 (2010) 3813-3821.

[8] L. Zheng, M. Zhang, J. Dong, Oxidation behavior and mechanism of powder metallurgy Rene95 nickel based superalloy between 800 and 1000 °C, Applied Surface Science, 256 (2010) 7510-7515.

[9] M.P. Taylor, H.E. Evans, S. Stekovic, M.C. Hardy, The oxidation characteristics of the Ni-base superalloy, RR1000, at temperatures 700-900^{o}C, Materials at High Temperatures, 29 (2012) 145-150.

[10] S. Cruchley, M.P. Taylor, H.E. Evans, D.J. Child, M.C. Hardy, Characterisation of the Sub-surface Oxidation Damage in the Ni-based Superalloy, RR1000, Materials Science and Technology - 30 (2014) 1884-1889.

[11] S. Cruchley, H.E. Evans, M.P. Taylor, M.C. Hardy, S. Stekovic, Chromia layer growth on a Ni-based superalloy: Sub-parabolic kinetics and the role of titanium, Corrosion Science, 75 (2013) 58-66.

[12] A. Encinas-Oropesa, G.L. Drew, M.C. Hardy, A.J. Leggett, J.R. Nicholls, N.J. Simms, Effects of oxidation and hot corrosion in a nickel disc alloy, in: Superalloys 2008: 11th International Symposium on Superalloys TMS, (2008), 609-618.

[13] A. Encinas-Oropesa, N.J. Simms, J.R. Nicholls, G.L. Drew, J. Leggett, M.C. Hardy, Evaluation of oxidation related damage caused to a gas turbine disc alloy between 700 and 800°C, Materials at High Temperatures, 26 (2009) 241-249.

[14] R.J. Mitchell, C.M. Rae, S. Tin, Grain boundary transformations during isothermal exposure of powder metallurgy nickel base superalloys for turbine disc applications, Materials Science and Technology, 21 (2005) 125-132.

[15] L. Tan, X. Ren, K. Sridharan, T.R. Allen, Effect of shot-peening on the oxidation of alloy 800H exposed to supercritical water and cyclic oxidation, Corrosion Science, 50 (2008) 2040-2046.

ACCEPTED MANUSCRIPT

[16] R. Naraparaju, H.J. Christ, F. Renner, A. Kostka, Effect of shot-peening on the oxidation behaviour of boiler steels, Oxidation of Metals, (2011) 1-13.

[17] S. Cruchley, M.P. Taylor, H.E. Evans, P. Bowen, M.C. Hardy, S. Stekovic, Microstructural Characterisation of High Temperature Oxidation of Nickel Base Superalloy RR1000 and the Effect of Shot-Peening, in: E.S. Huron, R.C. Reed, M.C. Hardy, M.J. Mills, R.E. Montero, P.D. Portella, J. Telesman (Eds.) Superalloys 2012: 12th International Symposium on Superalloys, TMS, Seven Springs, PA, 2012, pp. 751-758.

[18] A.N. Blacklocks, A. Atkinson, R.J. Packer, S.L.P. Savin, A.V. Chadwick, An XAS study of the defect structure of Ti-doped a-Cr_2O_3, Sol. State Ionics 177 (2006) 2939–2944.

[19] G.C. Wood, T. Hodgkiess, D.P. Whittle, A comparison of the scaling behaviour of pure iron-chromium and nickel-chromium alloys in oxygen, Corrosion Science, 6 (1966) 129-147.

[20] I.M. Edmonds, H.E. Evans, C.N. Jones, The role of γ′ precipitate dispersion in forming a protective scale on Ni-based superalloy at 750^{o}C, Oxidation of Metals, 73 (2012) 193-206.

[21] J. Issartel, S. Martoia, F. Charlot, V. Parry, G. Parry, R. Estevez, Y. Wouters, High temperature behavior of the metal/oxide interface of ferritic stainless steels, Corrosion Science, 59 (2012) 148-156.

[22] P. Huszkowski, S. Ertl, J. Piron-Abellan, N. Christiansen, T. fler, V. Shemet, L. Singheiser, W.J. Quadakkers, Effect of component thickness on lifetime and oxidation rate of chromia forming ferritic steels in low and high pO_2 environments, Materials at High Temperatures, 22 (2005) 253-262.

[23] H. Ackermann, G. Teneva-Kosseva, K. Lucka, H. Koehne, S. Richter, J. Mayer, Oxidation behaviour of selected wrought Ni-base high temperature alloys when used as flame tube material in modern blue flame oil burners, Corrosion Science, 49 (2007) 3866-3879.

[24] D.J. Young, Predicting internal oxidation: Building on the wagner model., Materials Science Forum, 969 (2011) 1-11.

[25] G.V. Samsonov, The oxide handbook, 2nd Edition ed., IFI/Plenum, New York and London, 1982.

[26] H.E. Evans, D.A. Hilton, R.A. Holm, S.J. Webster, Influence of a titanium nitride dispersion on the oxidation behaviur of 20%Cr 25%Ni stainless steel, Oxidation of Metals, 12 (1978) 473-485.

[27] A. Atkinson, M.R. Levy, S. Roche, R.A. Rudkin, Defect properties of Ti-doped Cr_2O_3, Solid State Ionics, 177 (2006) 1767-1770.

[28] A.N. Blacklocks, A. Atkinson, R.J. Packer, S.L.P. Savin, A.V. Chadwick, An XAS study of the defect structure of Ti-doped α-Cr_2O_3, Solid State Ionics, 177 (2006) 2939-2944.

[29] P.J. Ennis, W.J. Quadakkers, Corrosion and creep of nickel-base alloys in steam reforming gas, in: J.B. Marriott, M. Merz, J. Nihoul, J. Ward (Eds.) High Temperature Alloys, Springer Netherlands, 1988, pp. 465-474.

[30] H. Buscail, S. Perrier, C. Josse, Oxidation mechanism of the Inconel 601 alloy at high temperatures, Materials and Corrosion, 62 (2011) 416-422.

[31] A. Holt, P. Kofstad, Electrical conductivity of Cr_2O_3 doped with TiO_2, Solid State Ionics, 117 (1999) 21-25.

ACCEPTED MANUSCRIPT

Table captions:
Table I: Nominal composition of RR1000 in atomic and weight %.

Table II: Test matrix showing exposure times at which specimens were removed for examination. All tests were performed in laboratory air.

Table III: XRD results of specimens held at 700^{o}C, 750^{o}C and 800^{o}C, with and without shot-peening, illustrating which oxides form. Identification was performed over a 2θ of 10-100^{o}.

Table IV: Growth kinetic rate constants and exponent for the external chromia layer on RR1000 in both the polished and shot-peened conditions and chromia growth on a high Cr austenitic steel.

Figure Captions:

Figure 1: BSE images of a cross-section through a) a polished RR1000 sample and b) a shot-peened RR1000 sample both oxidised at 700^{o}C for 2000 hours. Both show a continuous external scale of chromia, with sub-surface alumina penetration into the alloy. The figure also illustrates how the chromia measurements were performed.

Figure 2: a) SEM image, with energy dispersive X-ray analysis maps, of a section through a shot-peened RR1000 sample held in laboratory air at 800°C for 500 hours. b) SEM image, EDS point analysis of Ta-Ti rich phase formed underneath the external oxide scale oxidised at 800^{o}C for 2000 hours.

Figure 3: STEM image with EDS elemental analysis of a TEM foil taken from a specimen oxidised at 800^{o}C for 2000 hours, identifying the unknown phase as being rich in Ti, Ta and O.

Figure 4: Selected area electron diffraction patterns for the [10 $\bar{1}$], [100] and [3 $\bar{1}\bar{1}$] orientations for the Ta, Ti rich oxide.

ACCEPTED MANUSCRIPT

Figure 5: Secondary electron (SE) images produced using a focussed ion beam (FIB) of a cross-section of a shot-peened RR1000 sample oxidised for 200 hours at 800^{o}C illustrating recrystallised grains in the γ' denuded zone.

Figure 6: Plot of chromia thickness measured on RR1000, with and without shot-peening, at 700^{o}C, 750^{o}C and 800^{o}C compared with Ti-free austenitic steel/pure chromia. Oxide measurements for both conditions were normally distributed and error bars are shown as ± 1 standard deviation. Hollow squares are measurements for shot-peened RR1000, filled circles are polished RR1000.

Figure 7: The variation of the enhancement ratio with oxide thickness for 700^{o}C, 750^{o}C and 800^{o}C, in a) polished RR1000 and b) shot-peened RR1000.

Figure 8: EDS linescan (and BSE images) of polished RR1000 oxidised isothermally at 750^{o}C for a) 100 hours and b) 2000 hours showing titanium and aluminium depletion underlying the external oxide scale.

Figure 9: EDS linescan (and BSE images) of shot-peened RR1000 oxidised isothermally at 750^{o}C for a) 100 hours and b) 2000 hours showing titanium and aluminium depletion underlying the external oxide scale.

Figure 10: EDS linescan (and BSE images) of polished RR1000 oxidised isothermally at 800^{o}C for a) 100 hours and b) 2000 hours showing titanium and aluminium depletion underlying the external oxide scale.

Figure 11: EDS linescan (and BSE images) of shot-peened RR1000 oxidised isothermally at 800^{o}C for a) 100 hours and b) 2000 hours showing titanium and aluminium depletion underlying the external oxide scale.

Please include colour images for the online version only – greyscale images will be provided for the print version.

Table I

ACCEPTED MANUSCRIPT

Table II

		Ni	Co	Cr	Mo	Ti	Al	Ta	Hf	Zr	C	B
				224h		100h	100h	500h	500h	0h		2000h
Weight %		Bal	13.5	15.0	5.0	3.0	3.0	2.0	0.5	0.05	0.02	0.03
Shot-peened	700ºC	Bal	17.9	16.5	3.0	4.3	3.35	0.63	TiO_2 & Cr_2O_3	0.04	0.14	TiO_2 & Cr_2O_3
Atomic %									0.10			0.10
	750ºC		x	-	x	TiO_2 & Cr_2O_3			TiO_2 & Cr_2O_3			TiO_2 & Cr_2O_3
	800ºC		TiO_2 & Cr_2O_3		x	TiO_2 & Cr_2O_3			TiO_2 & Cr_2O_3			TiO_2 & Cr_2O_3 & $NiCr_2O_4$ (tr)
Polished	700ºC		x		x		x		x			x
Polished	700ºC			-			-		TiO_2 & Cr_2O_3			TiO_2 & Cr_2O_3
	750ºC		x		x		x		x			x
	750ºC			-		TiO_2 & Cr_2O_3			TiO_2 & Cr_2O_3			TiO_2 & Cr_2O_3
	800ºC		x		x		x		x			x
	800ºC		TiO_2 & Cr_2O_3			TiO_2 & Cr_2O_3			TiO_2 & Cr_2O_3 & $NiCr_2O_4$ (tr)			TiO_2 & Cr_2O_3 & $NiCr_2O_4$ (tr)

Table III

Table IV

Temperature	Shot-peened RR1000		Polished RR1000		Pure chromia formation	
	1/m	k_m ($\mu m^{1/m}.s^{-1}$)	1/m	k_m ($\mu m^{1/m}.s^{-1}$)	1/m	k_m ($\mu m^{1/m}.s^{-1}$)
700ºC	0.311	8.48×10^{-7}	0.340	5.63×10^{-7}	0.5	2.94×10^{-8}
750ºC	0.299	2.71×10^{-6}	0.327	9.16×10^{-7}	0.5	1.40×10^{-7}
800ºC	0.343	1.68×10^{-5}	0.477	8.81×10^{-6}	0.5	5.75×10^{-7}

Figure 1

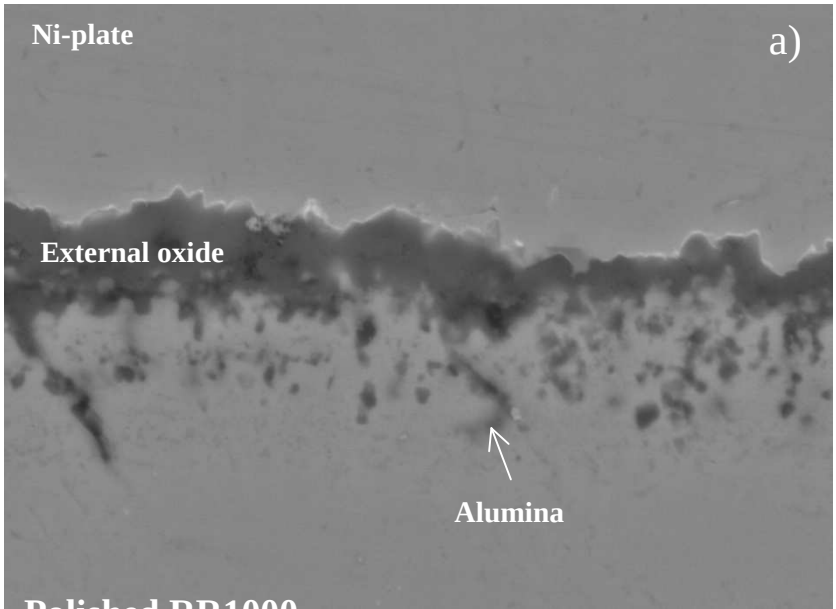

ACCEPTED MANUSCRIPT

Figure 2

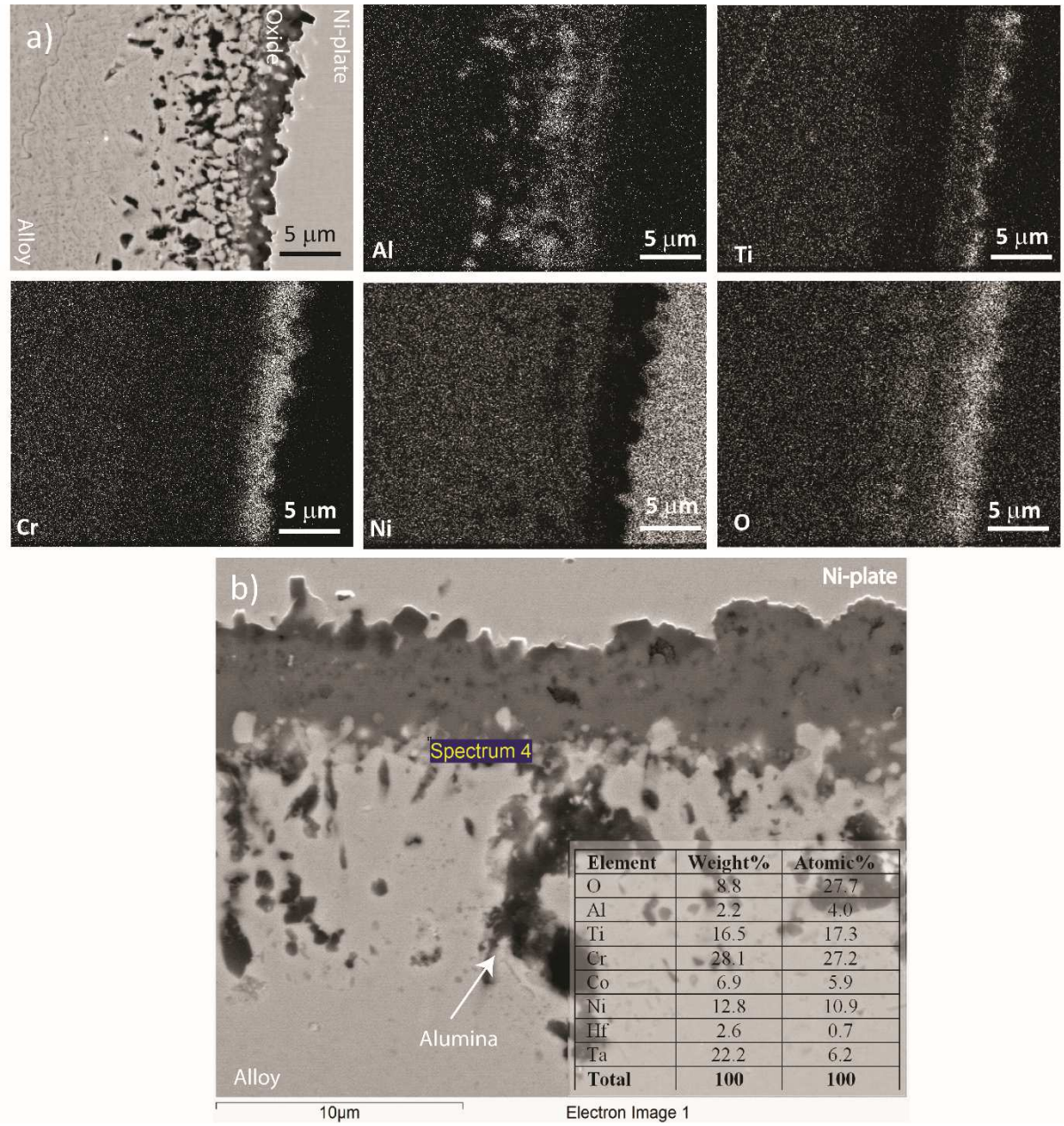

Element	Weight%	Atomic%
O	8.8	27.7
Al	2.2	4.0
Ti	16.5	17.3
Cr	28.1	27.2
Co	6.9	5.9
Ni	12.8	10.9
Hf	2.6	0.7
Ta	22.2	6.2
Total	**100**	**100**

Figure 3

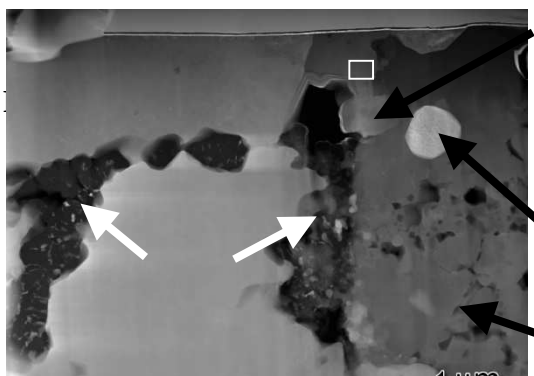

Unidentified phase

Element	Atomic%
O	63.2
Ti	20.6
Cr	4.2
Ta	12.0
Total	**100**

Entrapped alloy

Surface oxide

ACCEPTED MANUSCRIPT

Figure 5

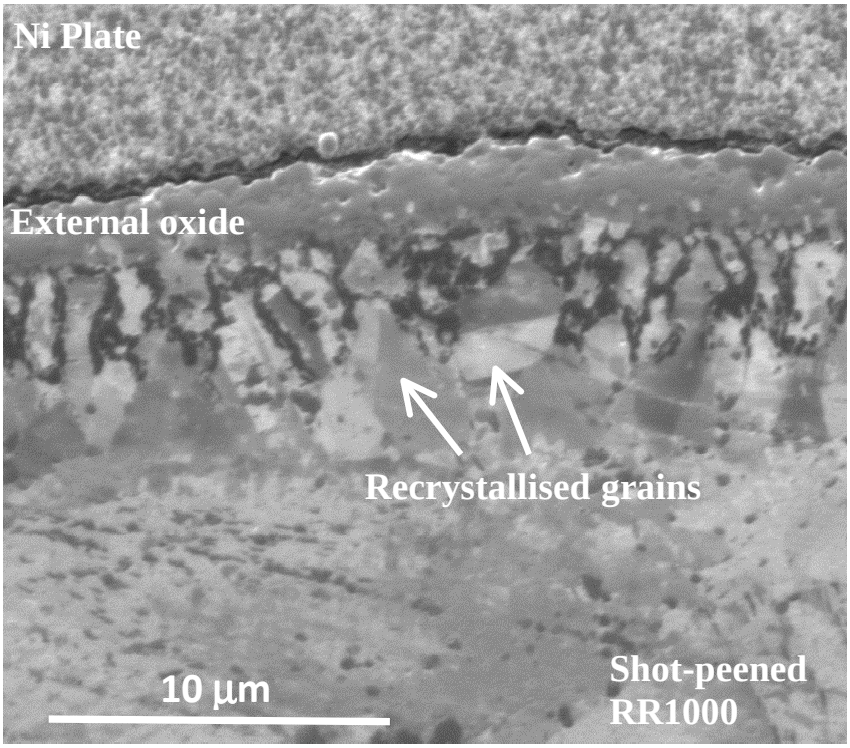

Figure 6

Figure 7

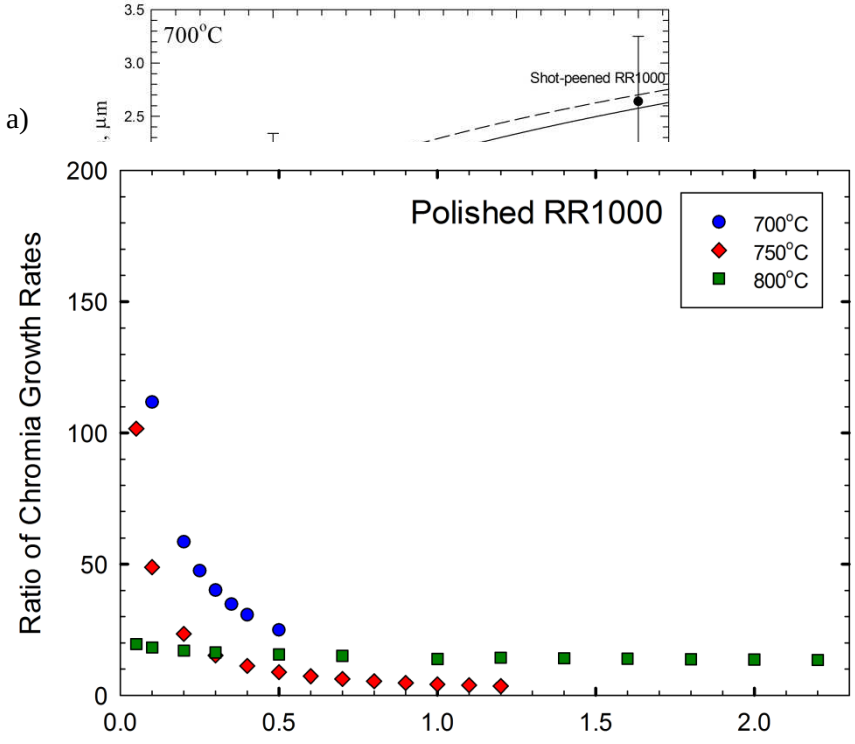

Figure 8

ACCEPTED MANUSCRIPT

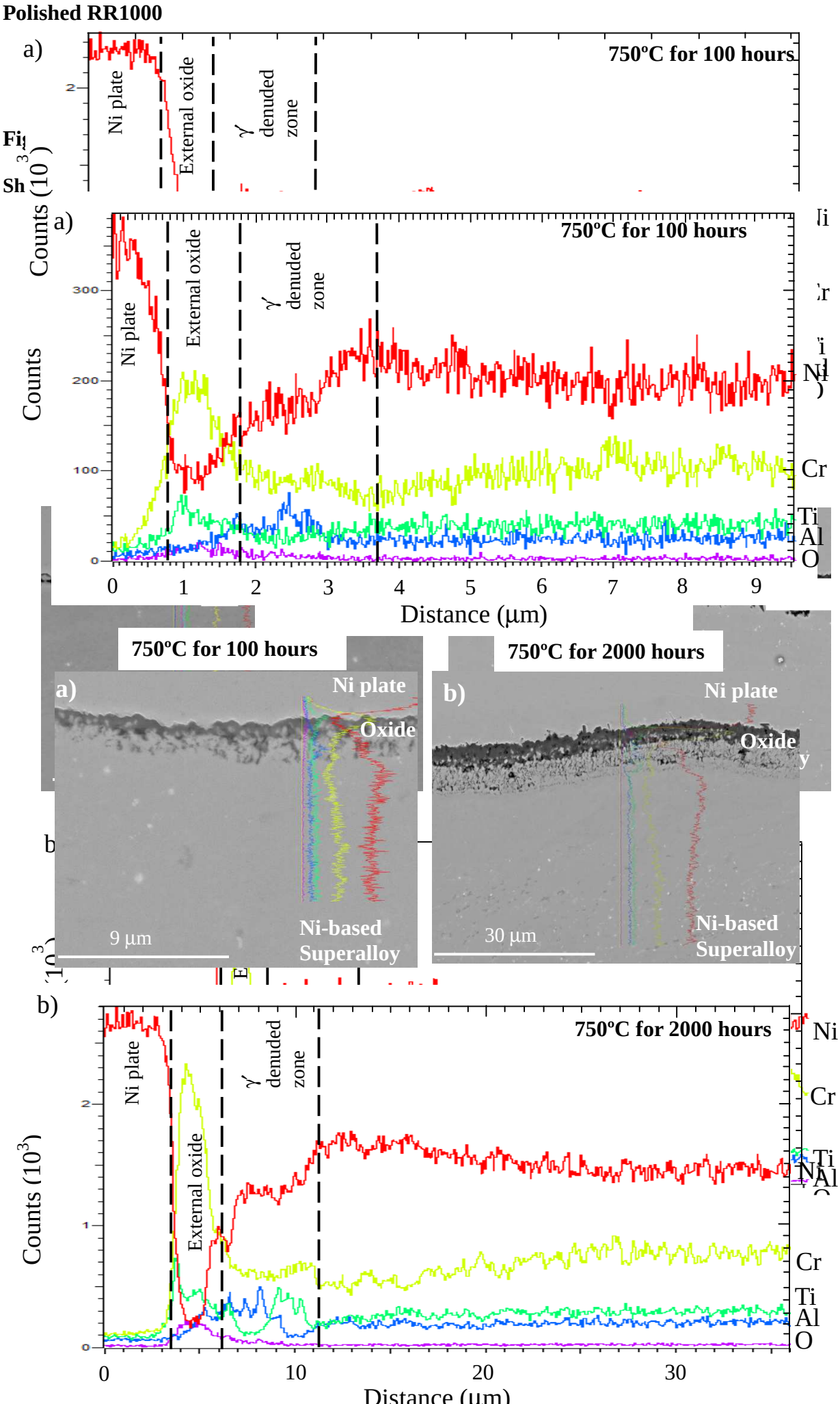

ACCEPTED MANUSCRIPT

Figure 10

Polished RR1000

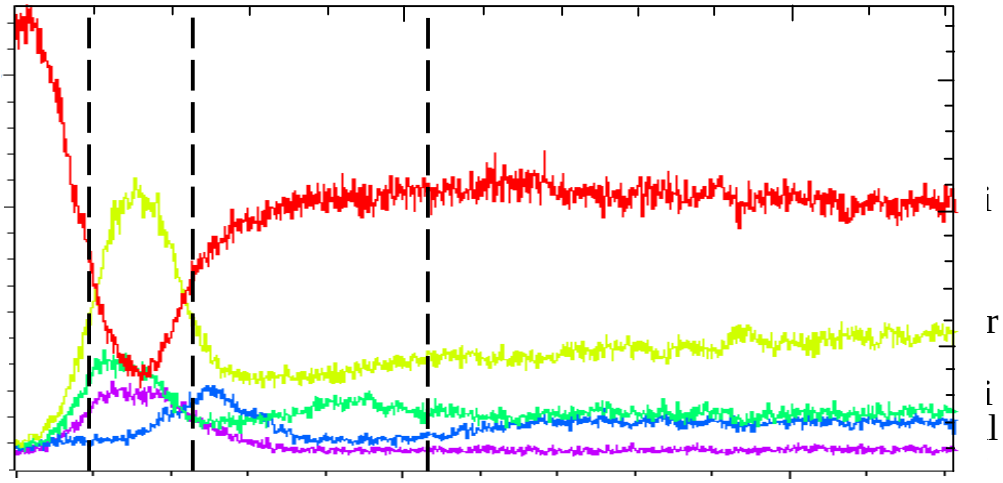

800°C for 200 hours

800°C for 2000 hours

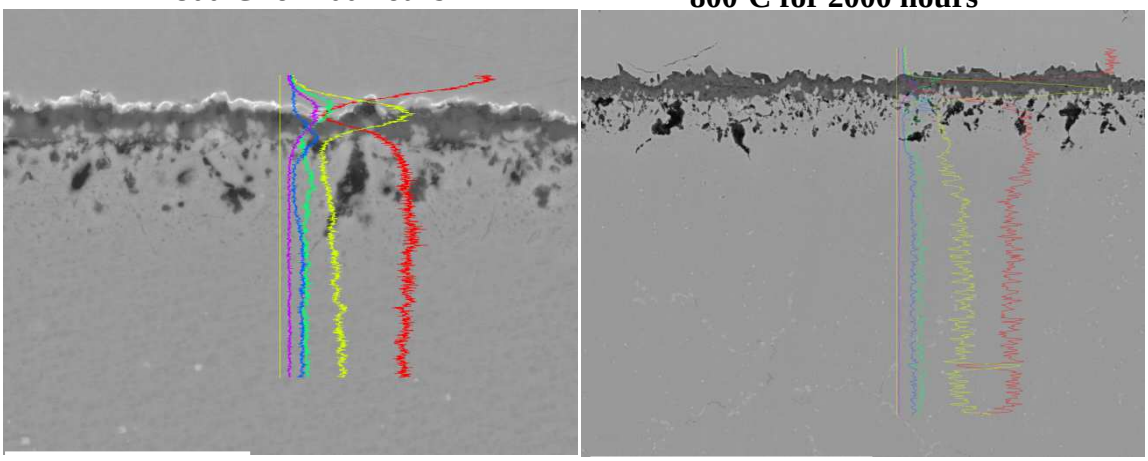

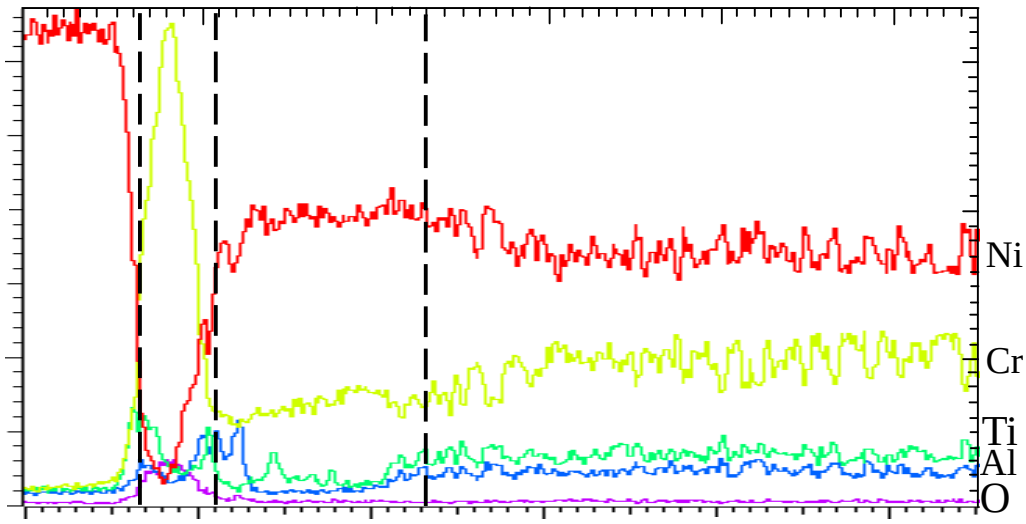

ACCEPTED MANUSCRIPT

Figure 11

Shot-peened RR1000

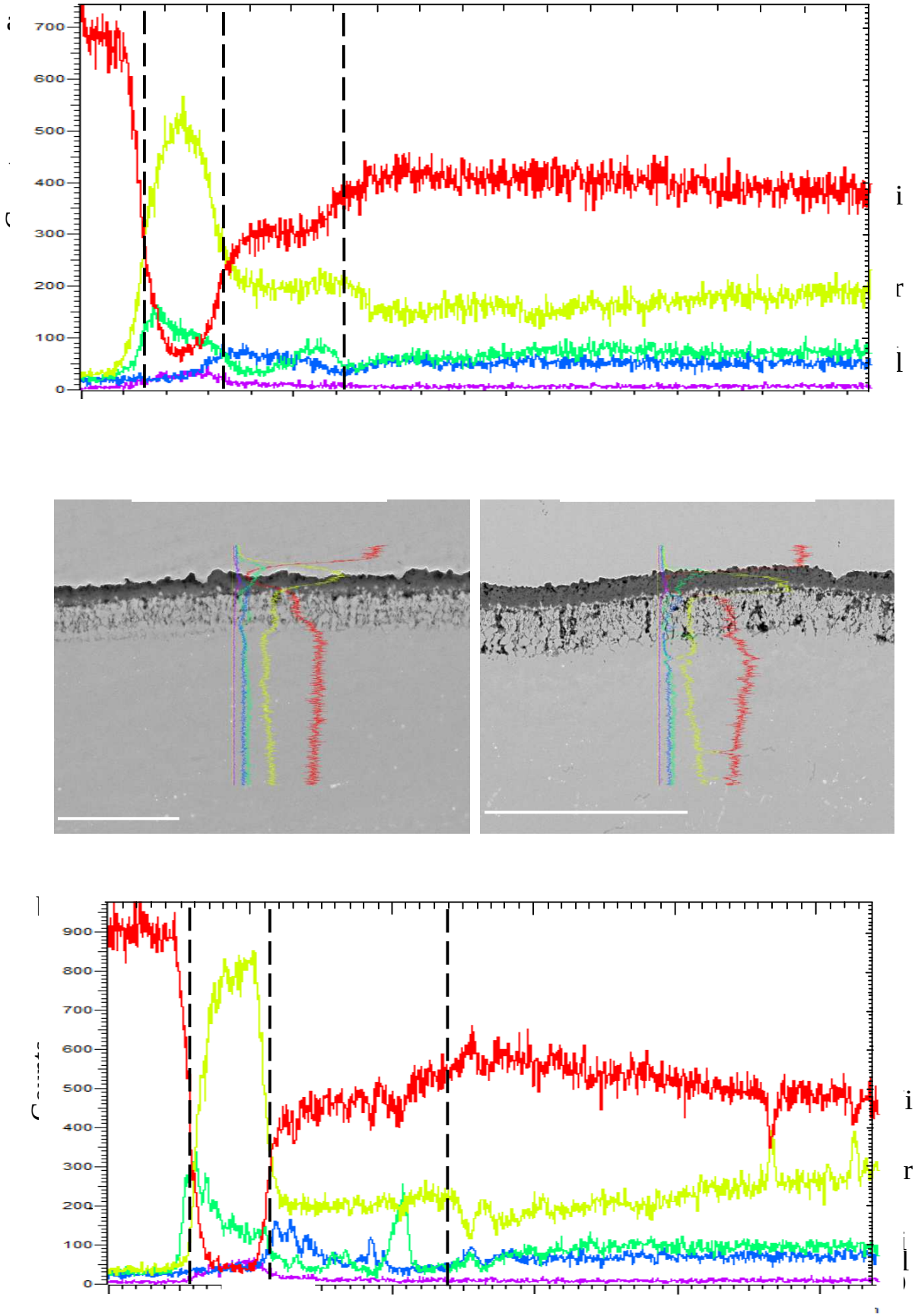

ACCEPTED MANUSCRIPT

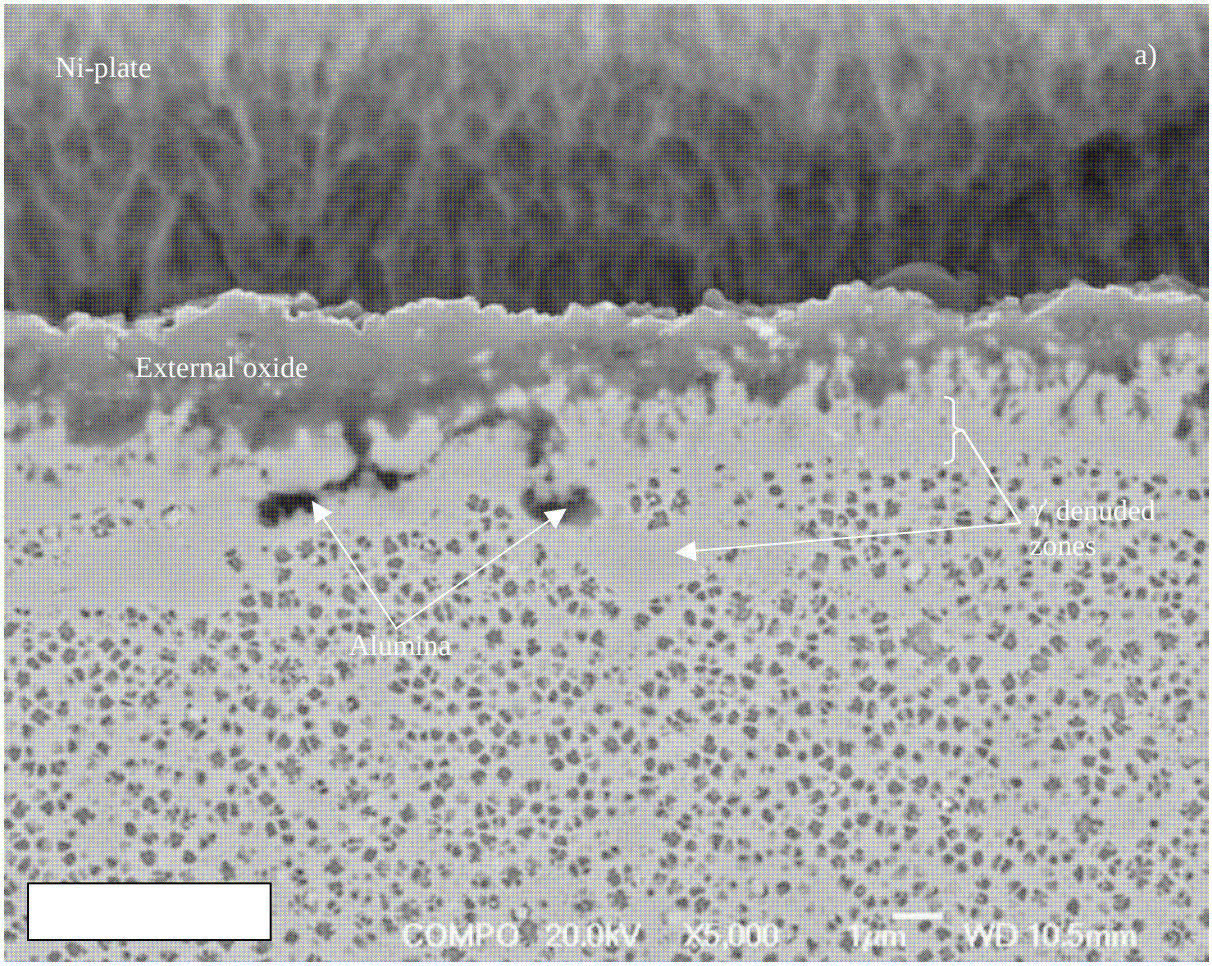

ACCEPTED MANUSCRIPT

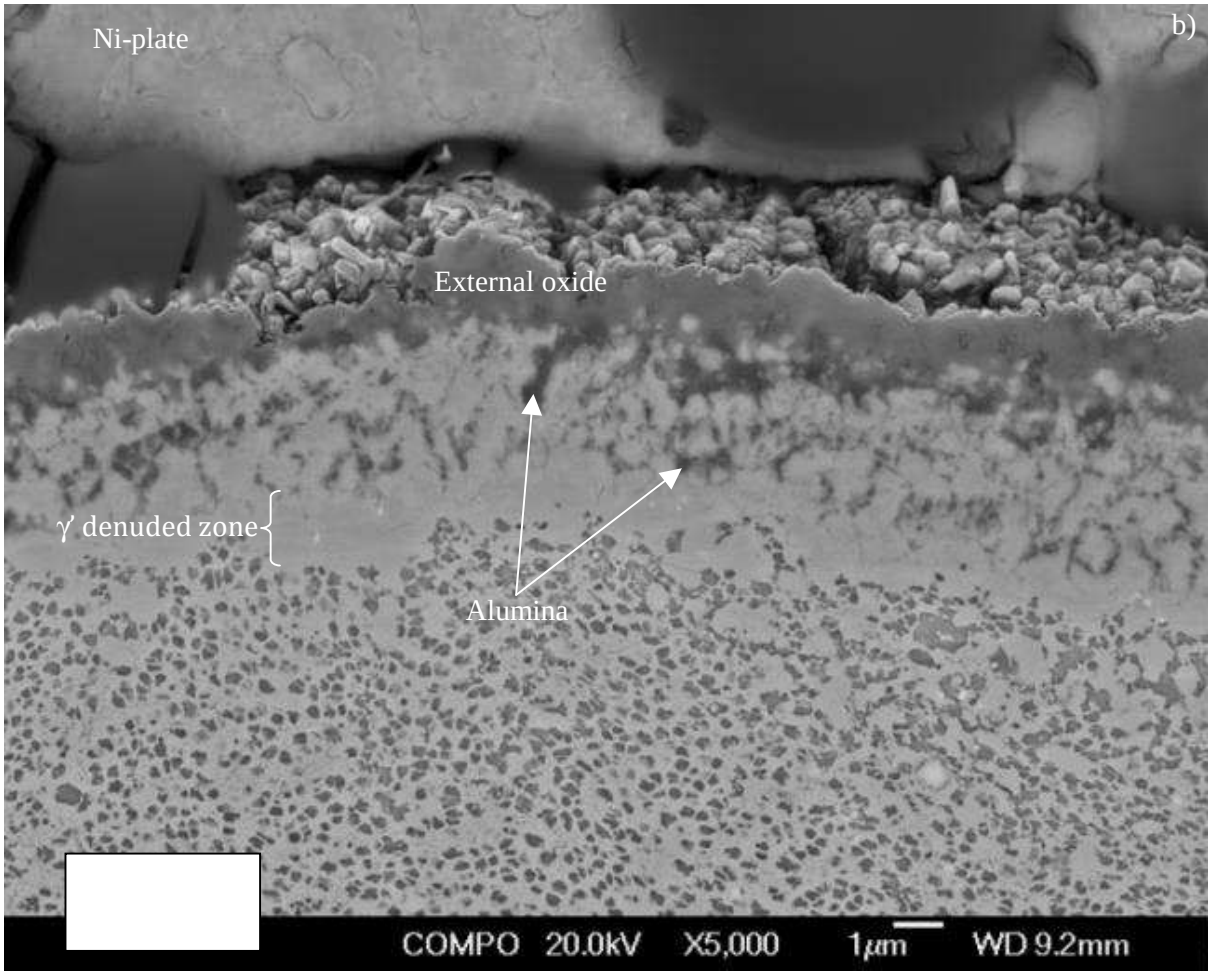

RR1000 shot peened, 2000h/700°C

ACCEPTED MANUSCRIPT

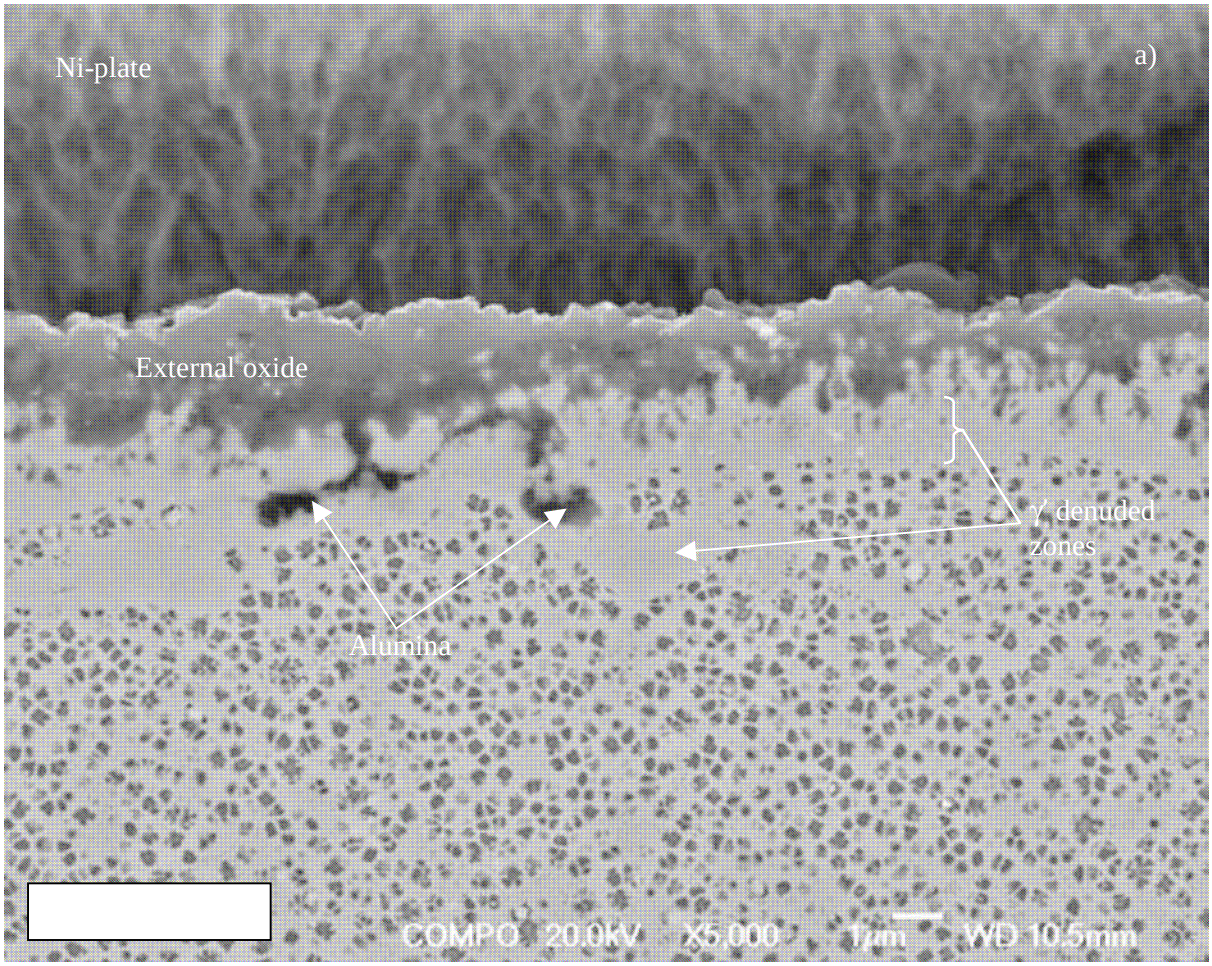

ACCEPTED MANUSCRIPT

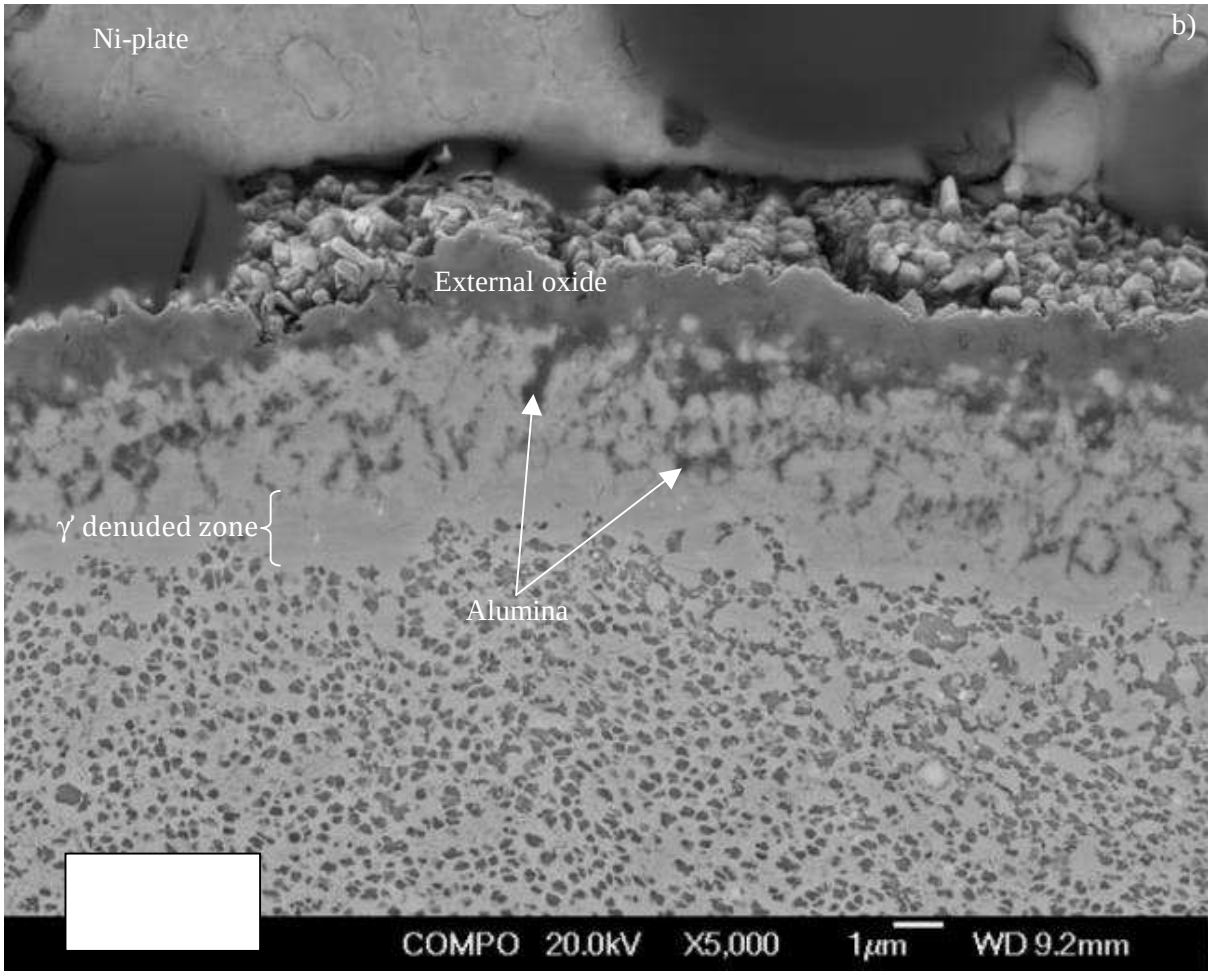

RR1000 shot peened, 2000h/700°C